Downloaded from

The version of record is available from

This document version

Author's Accepted Manuscript

DOI for this version

Licence for this version

Additional information

Versions of research works

Versions of Record

Author Accepted Manuscripts

Enquiries

Dual-Polarized and Wide-Angle Scanning Microstrip Phased Array

Ya-Qing Wen, Steven Gao, Bing-Zhong Wang,
Senior Member, IEEE and Qi Luo

Abstract—In this paper, a novel microstrip phased array with dual-polarized and wide-angle scanning in the 2-dimensional (2D) space is proposed. The antenna element consists of a mushroom-shaped patch and two circular patches. Each circular patch is connected with one feeding port. The mushroom-shaped patch is excited via capacitive coupling through the gaps between the mushroom-shaped patch and the circular patch. The zeroth-order resonance (ZOR) and TM_{010} mode resonance are simultaneously generated in the mushroom-shaped patch. The 3dB beamwidth of the antenna element in the 2D space is in the range between $110°$ and $125°$. One 6×6 phased array based on the antenna element is designed, fabricated and measured. The phased array shows dual-polarized wide-angle beam scanning in a range of $\pm66°$ in both *x-z* and *y-z* planes.

Index Terms—**Microstrip antenna, phased array, wide-angle scanning, dual-polarization**

I. INTRODUCTION

PHASED arrays have been widely used in the military radar and civilian satellite communications, etc., because they electronically scan the beam without any mechanical movement [1]-[2]. In recent years, it becomes increasingly important for researchers to investigate the technique of extending the beam scanning angle range of phased arrays and related beamforming technology. One of the popular techniques of achieving wide-angle beam scanning is to broaden the 3dB beamwidth of the antenna elements in phased arrays, such as the use of pattern reconfigurable elements [3]-[5] where the total scanning area was divided into several sub-areas with different radiation modes of the element antennas. The gain of the elements was kept large enough in the whole scanning range, which is an effective way to extend the 3dB beamwidth of the elements. The corresponding phased array using such reconfigurable elements extended the scanning angle range to more than $\pm70°$.

Mutual coupling between antenna elements is one important factor causing limited range of beam scanning. Strong mutual coupling between antenna elements leads to deterioration of antenna gain, sidelobe and efficiency at large scan angles. One important technique to achieve wide-angle beam scanning is to reduce the mutual coupling between antenna elements [6]. On the other hand, the mutual coupling can also be utilized in the phased array. In [7], the author presented a patch antenna with multiple ports. The active elements were directly fed from ports of feeding network, while the parasitic elements were excited by coupling energy from coupling ports of the active element. Applying this three-element patch subarray, a low-cost phased array is realized.

It is important to for a phased array to have stable polarization. In the linear phased array, normally vertically polarized radiation pattern is applied [8]-[11]. Endfire lobes can be generated by vertically polarized radiation pattern with an infinite ground. It is helpful for the wide-angle scanning and phased array with angle scan range over $\pm77°$ at the elevation plane was reported in [11]. Dual-polarized antennas have been required for phased arrays to be applied to various applications such as mobile satellite communications, weather radars, and synthetic aperture radars [12], [13]. The dual-polarized radiation can enhance the transmission efficiency between the transmitted and received antennas. Techniques to obtain dual-polarization includes using multiport feeding and multimode operating [14]-[17]. In the reference [18], in order to realize a differential feed, the dual-polarized patch antenna was excited by two tapered baluns, thus achieving a high isolation (higher than 28 dB) and reduced cross-polarization levels.

While the dual-polarized antenna operated in the phased array, some serious problems need to be solved. The stability of the polarization and the isolation between the orthogonal polarizations are especially critical. A dual-polarized suspended stripline fed open-ended waveguide antenna subarray was proposed and applied in a phased array in [19]. In order to keep a good isolation between the two polarized ports, multilayer configuration was used. There was a compact transition between the waveguide and the suspended stripline, and the cross polarization level of the antenna was less than -27 dB. Waveguide antenna and Vivaldi antenna were applied as the antenna element in the dual-polarized phased array in the reference [20] and [21]. For the waveguide antenna, dual-ports were used to obtain the dual-polarized radiation. For the Vivaldi antenna, double-mirror balanced antipodal Vivaldi antennas reversed along the E- and H- planes as elements. The double-mirroring can be employed for dual-polarized radiation in the array. Both phased arrays can scan their beams with dual-polarization over $\pm40°$.

This paper presents the designs of a microstrip antenna and a phased array. A novel array element with wide beamwidth is developed by letting the microstrip antenna simultaneously operates in ZOR mode and TM_{010} mode at the frequency of interest. The microstrip antenna with only TM_{010} mode cannot obtain wide beamwidth. However, the microstrip antenna with ZOR mode radiates like a monopole, which has a radiation beam at the low angles in the elevation plane and a radiation null pointing in the vertical direction. Therefore, the combination of the ZOR mode and the TM_{010} mode can realize an antenna with wide beamwidth [22]. The dual-LP radiations are obtained by using two feeding ports on the antenna, one is for *x*-polarization and the other is for *y*-polarization. The microstrip phased array designed by using this element can scan its main lobe within a wide-angle range in the 2D space.

II. THE MICROSTRIP ANTENNA OPERATED WITH ZOR MODE AND TM_{010} MODE

A. The Structure of the Microstrip Antenna

The structure of the antenna is shown in Fig. 1. The antenna is printed on a dielectric substrate with a size of $La \times Lb$. The substrate is F4B-2 with a thickness of 2mm, $\varepsilon_r = 2.65$, and $\delta_d = 1.9 \times 10^{-3}$. A rectangular patch is printed on the top of the substrate, while the bottom of the substrate is the ground plane. The antenna element is mushroom-shaped as there is a metal via connecting the center of the rectangular patch to the metal ground. Two circular patches of the same size are inserted on the adjoining edges of the rectangular patch. Coaxial probes with characteristic impedance 50Ω are connected to the center of the circular patches. There is a gap (s) between the circular patch and the rectangular patch, so the excited energy is transmitted from the circular patches to the mushroom-shaped patch via capacitive coupling. The specific parameters of the antenna are as follow: $La=Lb=80$ mm; $Wa=Wb=15.5$ mm;

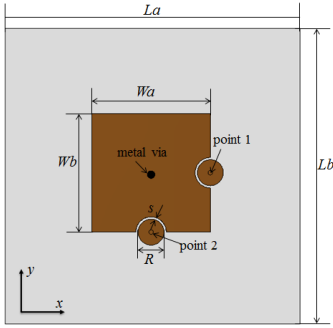Fig. 1. Structure of the proposed microstrip antenna
$R=1.7$ mm; $s = 0.3$ mm.

B. The ZOR Mode and TM_{010} Mode

The TM_{010} mode can be generated in the proposed antenna as a conventional rectangular patch antenna. The electric fields distributions inside the patch are shown in Fig. 2. It is well known that the half-wavelength wave is generated inside the antenna and the resonance frequency is decided by the length of the patch's edge with half-period field. In order to keep the same resonance frequency generated with the two different ports, a square rectangular patch was selected.

In the center of the square rectangular patch, there is a metal via which connected the patch to the ground plane. The patch has been a shape of a mushroom. In general, the mushroom-shaped antenna can work with an infinite wavelength mode at a specific non-zero frequency called a ZOR mode. The radiation of antenna with ZOR mode is like one of the monopoles. The size of the patch, the radius of the via, the thickness of the substrate, and the size of the metal ground have an influence on the radiation. The mushroom-shaped patch with TM_{010} mode and ZOR mode has an equivalent circuit [23] as shown in Fig. 3, when Port 1is excited.

In the equivalent circuit, Lf is the inductance generated by the feeding probe and Cf is the capacitance generated by the circular patch. Cs is the capacitance of the gap between the circular patch and the rectangular patch. For the mushroom-
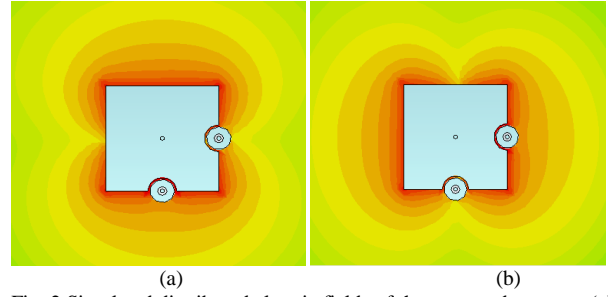

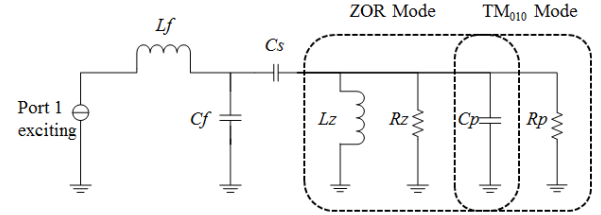Fig. 2 Simulated distributed electric fields of the proposed antenna, (a) port 1 excited; (b) port 2 excited

Fig. 3. Equivalent circuit of the mushroom patch when excited by one port

shaped patch, Cp and Rp are, respectively, the shunt capacitance and shunt resistance generated by the patch and the metal ground. Lz and Rz are, respectively, shunt inductance and shunt resistance generated by the via. They connected the source by the series capacitance Cs.

The antenna should obtain a wide beamwidth radiation pattern, with a combination of the ZOR mode and TM_{010} mode. The radiated power between the ZOR mode and TM_{010} mode should be balanced. The details will be discussed in Section III.

III. WIDE BEAMWIDTH AND DUAL-POLARIZED RADIATION PATTERN OF THE ANTENNA

A. Wide 3dB Beamwidth of the Radiation Pattern

It is known that a microstrip antenna with ZOR mode has a conical-shaped radiation pattern, like a monopole's dominant mode. The radiation null arises at the vertical direction ($\theta=0°$ of the z-axis). The radiation pattern on the horizontal plane (x-y plane) is omnidirectional. The direction of the main lobe at the elevation plane is decided by the size of the metal ground. The pointing angle becomes lower as the metal ground being smaller. On the other hand, the microstrip antenna with only TM_{010} mode has a radiation pattern with the main lobe toward the vertical direction. The combination of the ZOR mode and the TM_{010} mode makes combined radiation pattern with wide coverage.

Fig.4 shows the radiation patterns of the antenna with only TM_{010} mode when Port 1 is excited. In this case, there is no via in the center of the patch. The radiation is the same as that of the conventional rectangular patch. The change of the size of metal ground has little influence on the radiation pattern. The radiation patterns at both x-z plane and y-z plane are linear polarization, and the 3dB beamwidth of the radiation patterns is in the range of [77°, 85°].

When the ZOR mode is introduced by adding a central via, the antenna is configured to the proposed structure. Fig. 5 shows the simulated radiation patterns of the proposed antenna with different sizes of metal ground. The size of the metal ground has much influence on the radiation of ZOR mode. When the size is too small, the main lobe of the ZOR mode radiates around the low angles at the elevation plane, and the radiation interspace at the vertical angles is too much. In this case, the combination of ZOR mode and TM_{010} mode leads to a wave-shaped radiation pattern like the patterns in Fig. 5 when $La=Lb=40$mm. Similarly, when the metal ground is too large, the main lobe of ZOR mode can only radiate in the vertical direction. In this case, the combination of ZOR mode and TM_{010} mode cannot play the role of increasing the beamwidth. As shown in Fig. 5, when $La=Lb=120$ mm, the beamwidth of the radiation patterns are the same as those of only TM_{010} mode. Therefore, an optimized size of the metal ground is important to broaden the beamwidth of the antenna. It is found that the combination is perfect when $La=Lb=80$mm. The radiated lobe of the TM_{010} mode fills up the interspace of the radiation pattern of the ZOR mode around the vertical direction. Besides, the conical-shaped radiation pattern of the ZOR mode fills up the low angles in the elevation plane. A wide 3dB beamwidth radiation pattern is generated.

Furthermore, the incident powers of the ZOR mode and the TM_{010} mode should be in a suitable ratio, otherwise undesired wave-shaped radiation pattern will be generated. For the ZOR mode and the TM_{010} mode, the incident powers are respectively,

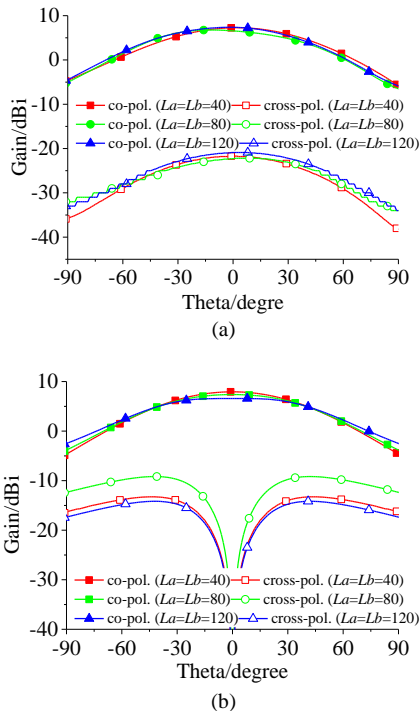$$P_{ZOR} = \frac{1}{2} R_z \cdot \left| i_z \right|^2 \tag{1}$$

Fig. 4. Simulated radiation pattern of the antenna with only TM_{010} mode (a) x-z plane; (b) y-z plane (only Port 1is excited, unit: mm)
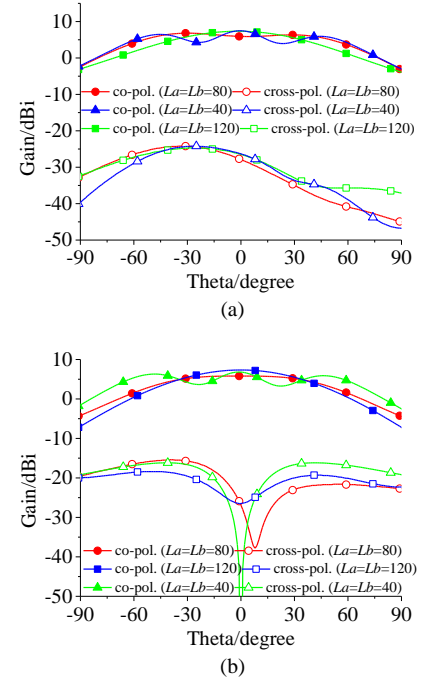
Fig. 5. Simulated radiation pattern of the antenna with ZOR mode and TM_{010} mode (a) x-z plane; (b) y-z plane (only Port 1is excited, unit: mm)

$$P_{TM_{010}} = \frac{1}{2} R_p \cdot \left| i_p \right|^2 \tag{2}$$

The incident powers are influenced by Rz and Rp directly, which are decided by the size of the metal via and thickness of the substrate. Tables I and II show the values of the 3dB beamwidth of the antenna with different radius of metal via and thickness of the substrate.

By comparing the results, the radius of the metal is set to 0.3mm, and the thickness is set to 2mm. With this configuration, the 3dB beamwidth of the antenna in both x-z and y-z planes are broadened.

B. Dual-Polarized Radiation Pattern of the Antenna

TABLE I
BEAMWIDTH OF THE ANTENNA WITH DIFFERENT VALUES OF METAL VIA'S RADIUS (ONLY PORT 1 IS EXCITED, SUBSTRATE'S THICKNESS IS 2MM)

R_{via} (mm)	0.1	0.3	0.5
3-dB BW (x-z plane)	81.6°	125.3°	99.2°
3-dB BW (y-z plane)	77.1°	110.0°	86.3°

TABLE II
BEAMWIDTH OF THE ANTENNA WITH DIFFERENT VALUES OF SUBSTRATE'S THICKNESS (ONLY PORT 1 IS EXCITED, METAL VIA'S RADIUS IS 0.3MM)

H (mm)	1	2	3
3-dB BW (x-z plane)	104.3°	125.3°	107.0°
3-dB BW (y-z plane)	89.5°	110.0°	100.2°

There are two feeding ports on the antenna. Fig. 6 shows the simulated current distribution with two ports excited, respectively. The surface currents point to the x-direction and y-direction, respectively. According to the antenna theory, the polarization of the radiation is decided by the surface currents on the radiating element. The x-direction-polarized radiation pattern is generated by the x-directional current. Similarly, the y-direction-polarized radiation pattern is generated by the y-
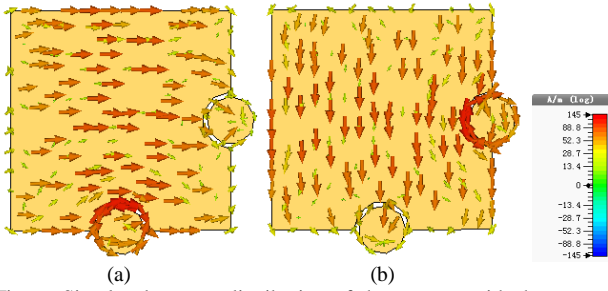
Fig. 6. Simulated current distribution of the antenna with the two ports excited successively, (a) Port 1 excited; (b) Port 2 excited

directional current. Therefore, the proposed antenna can obtain dual-polarized radiation patterns.

C. Measured Results and Analysis

The proposed antenna was fabricated and measured. The photos of the antenna porotype and the antenna under measurement are shown in Fig. 7.

Fig.8 shows the simulated and measured S-parameters of the two ports of the antenna. If there is no metal via, only TM_{010} mode is generated in the antenna. The resonance frequency is 5.23 GHz. While for the ZOR mode, the resonance is at 5.07 GHz. When two modes work together, the resonance is near 5.13 GHz in the simulation results. Because the antenna
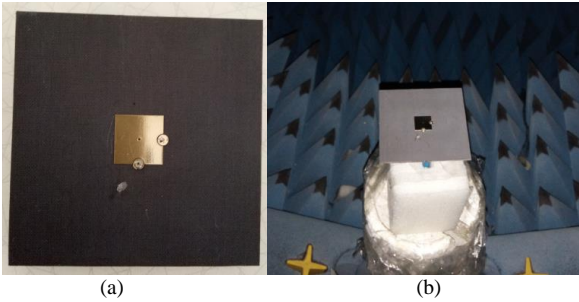

Fig.7. View of the antenna and measured scenarios in the anechoic chamber

structure is symmetrical, the simulated results of two ports are exactly the same, while the measured results show that the responses from the two ports are very similar. From Fig. 8, it can be seen that the simulated results show the overlapped bandwidth of the two polarizations from 5.02 GHz to 5.23 GHz, and the measured results show that the overlapped bandwidth of the two polarizations from 5.15 GHz to 5.26 GHz. Thus, the antenna can work with a bandwidth over 100MHz which is sufficient for some radar detection system. The isolation between the two ports is higher than 22 dB in its operating frequency band.
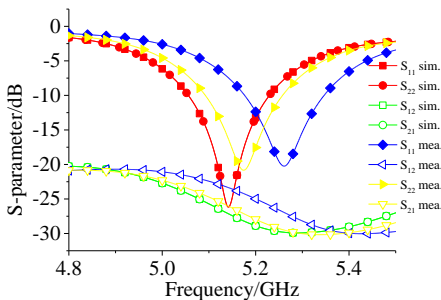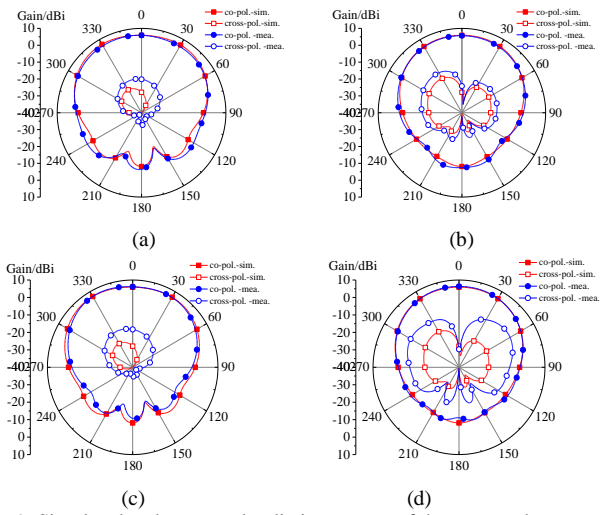

Fig.9. Simulated and measured radiation pattern of the proposed antenna. (a) Port 1 x-z plane; (b) Port 1 y-z plane; (c) Port 2 y-z plane; (d) Port 2 x-z plane.

Radiation patterns of the two ports are measured respectively at 5.2 GHz, which are shown in Fig. 9. During the measurement, when one port is excited, the other is connected to a matched load. When Port 1 is excited, the co-polarized radiation pattern is x-polarization at both x-z and y-z planes. The main lobe gain is 6.8 dBi, and the 3dB beamwidth is wider than 125° for the x-z plane and 110° for the y-z plane. Cross-polarized radiations of the simulated results are less than -21dBi. Because of the environmental noise, the cross-polarized radiations of the measured results are less than -16 dBi, which is larger than the simulated one.

Because of the symmetry, the radiation pattern with Port 2 excited is the same as that with Port 1 excited. The co-polarized radiation pattern is y-polarization at both x-z and y-z planes. The peak gain is 6.8 dBi, and the 3dB beamwidth is wider than 125° for the y-z plane and 110° for the x-z plane. The maximum cross-polarization of the measured results is less than -15 dBi. Therefore, the proposed antenna obtains a wide beamwidth radiation pattern in the upper space with dual-polarization.

IV. WIDE-ANGLE SCANNING IN THE UPPER SPACE

A 6×6 planar phased array was fabricated with the element antennas developed above. The view of the array measured in the anechoic chamber and the measurement system for the scanning radiation patterns are shown in Fig. 10. The measurement system was set-up by using coaxial cables, six-bit digital phase shifters, power dividers and a computer.
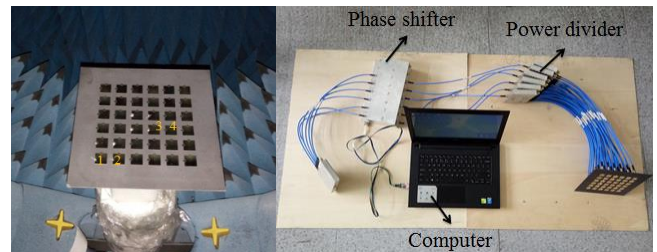

Fig. 8. Simulated and measured S-parameters of the proposed antenna

Fig.10. View of the phased array measured in the anechoic chamber and the measurement system

The distance between the adjacent elements is 23 mm. The size of the substrate is 19.5 cm×19.5 cm. Since the size of the metal ground plane has an effect on the radiation of the element antenna, the distance between the edge of the substrate and the edge elements is the same as the one on the single antenna, so the effect of the scattering of the edge of the metal ground is the same as that of the single antenna.
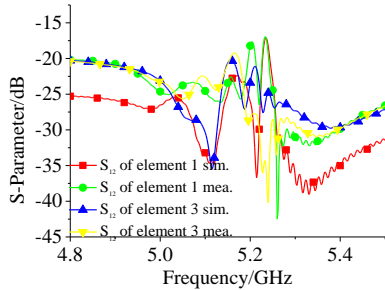

Fig.11. S21 and S12 of the two ports of orthogonal polarizations on Elements 1 and 3

As shown in Fig. 10, Elements 1 and 2 are the edge elements and Elements 3 and 4 are the middle elements. Fig. 11 shows the isolation between the two ports of orthogonal polarizations in Elements 1 and 3. Fig.12 shows the effect of the matching of Elements 1 and 3 with Port 1 excited, and the coupling between the adjacent elements with Port 1 excited. The elements have a perfect matching around 5.2 GHz with a bandwidth of 100 MHz. The S_{12} of the element's two ports in the array is less than -15 dB. The S_{12} between the adjacent elements is less than -16 dB.

Radiation patterns of Elements 1 and 3 in the x-z plane with Port 1 excited are shown in Fig.13. According to the analysis in Section III, a large size ground plane makes the beamwidth narrower than that of the single antenna. For the Element 3, the 3dB beamwidth is larger than 110°. For the edge Element 1 the lobe is inclined to one side and the 3dB coverage range can reach -70°in the elevation plane. Therefore, the beam of active
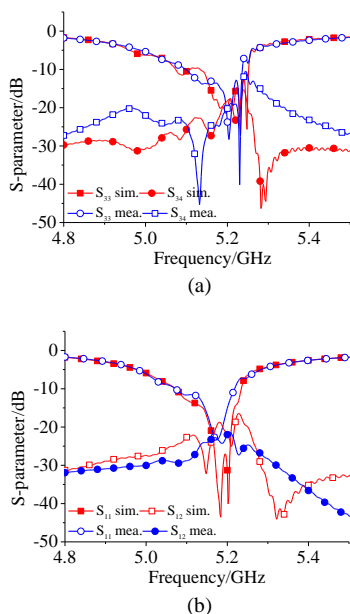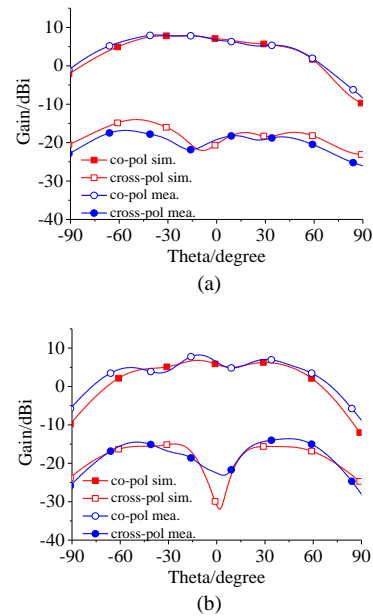

Fig.13. Active pattern of the element in the *x-z* plane with Port1 excited, (a) Element 1; (b) Element 3

patterns can also cover a wide angle range that is suitable for the wide angle scanning.

The scanning radiation patterns of the phased array were measured at 5.2 GHz. Fig. 14 shows the measured scanning radiation pattern in the x-z plane and y-z plane with Port 1 excited. Table III shows the specific scanning information from measurement of the phased array with Port 1 excited. In the table, "θ" is the main lobe direction in the elevation plane, "Gain" is the peak gain of the main lobe, "SLL" is the maximum sidelobe of the scanning pattern, and "Mcross-pol" is the maximum of the cross-polarization. Because of the
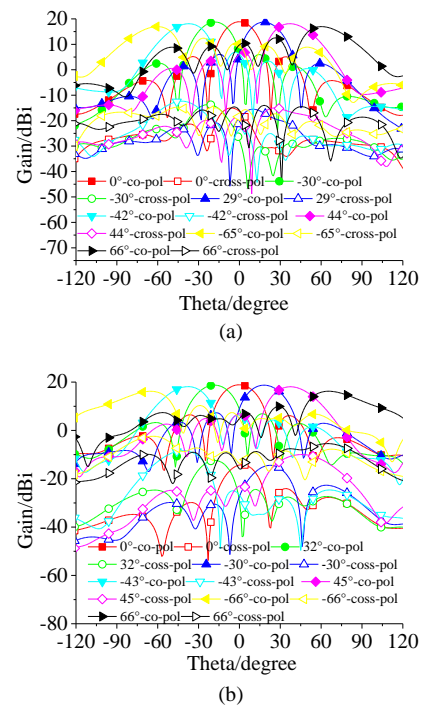

(a)

(b)

Fig.12. S-parameter of Elements 1 and 3,(a) Element 3;(b) Element1

(a)

(b)

Fig.14. Measured scanning radiation pattern of the phased array with Port 1 excited. (a) x-z plane; (b) y-z plane

TABLE III
SCANNING INFORMATION WHEN PORT 1 IS EXCITED

x-z plane			
θ (degree)	Gain(dBi)	SLL(dB)	Mcross-pol(dBi)
0	18.1	-15.8	-17.3
-30	17.8	-11.2	-14.6
29	17.2	-9.7	-14.8
-42	16.6	-12.2	-14.1
44	16.2	-9.6	-15
-65	15	-4.5	-14.4
66	14.7	-5	-14.8
y-z plane			
θ(degree)	Gain(dBi)	SLL(dB)	Mcross-pol(dBi)
0	18.1	-12.6	-17.3
-30	17.4	-12.2	-17.3
32	17	-11.5	-16.7
-43	16.1	-10.4	-16.5
45	15.4	-10.9	-15.9
-66	14.8	-5.8	-14.6

symmetry, the scanning radiation pattern and the scanning information when the Port 2 is excited are similar to the one with Port 1 excited. The co-polarization is x-pol when Port 1 is excited, and the co-polarization is y-pol when Port 2 is excited.

The phased array can scan its main lobe in a wide-angle range of ±66° in the y-z plane and a wide-angle range from -65° to 66° in the x-z plane. Meanwhile, the gain in the scanning range of the phased array is between 18.1 dBi and 14.6 dBi with a gain fluctuation of 3.5 dB. The SLL is less than -10dB in most scanning range. When the scanning lobes get the low elevation angle the SLL becomes larger because of the mismatching of the ports. The maximum SLL in the scanning range is less than -4.5 dB. When Port 1 and Port 2 are excited respectively, the x-polarization and y-polarization were generated. The amplitude of cross-polarization in the scanning range is less than -14.1dBi. The phased array shows a good dual-polarized scanning in a wide-angle range.

V. CONCLUSION

In this paper, a novel dual-polarized microstrip antenna with wide beamwidth is proposed. TM_{010} mode and ZOR mode are simultaneously excited so the radiation patterns of the two modes can be combined, which leads to wide beamwidth radiation patterns. The dual-LP is realized by exciting the microstrip patch with two ports through capacitive coupling, and the port isolation is higher than 22 dB. A 6×6 planar phased array is designed and fabricated using the developed array element. Dual-polarized beam scanning is realized in a wide-angle range of ±66° in both x-z and y-z planes.

REFERENCES

[1] R. J. Mailloux, *Phased Array Antenna Handbook*, Artech House Antennas and Propagation Library, 2nd ed., Norwood, MA, USA: Artech Print on Demand, 2008.

[2] C. A. Balanis, *Antenna Theory, Analysis and Design*, 2nd ed., New York, NY, USA: Wiley, 1997.

[3] S. Q. Xiao, M. C. Tang, Z. F. Ding, and B.-Z. Wang, "Wide-angle scanning phased array with pattern reconfigurable elements," *IEEE Trans. Antennas Propag.*, vol. 59, no. 11, pp. 4071-4076, Nov. 2011.

[4] Y. Y. Bai, S. Q. Xiao, B.-Z. Wang, and Z. F. Ding, "Applying weighted thinned linear array and pattern reconfigurable element to extend pattern scanning range of millimeter wave microstrip phased array," *J. Infrared, Milli. Terahertz Waves*, vol.31, no.1, pp.1-6, Jan. 2010.

[5] X. Ding, B.-Z. Wang, and G.-Q. He, "Research on a millimeter-wave phased array with wide-angle scanning performance," *IEEE Trans. Antennas Propag.*, vol. 61, no. 10, pp. 5319-5324, Nov. 2013.

[6] S.-W Qu, P.-F Li, R.-L Xia, S.-W Yang, J. Hu, Z.-P Nie, "Low-cost periodic sparse cavity-backed phased array based on multiport elements," *IEEE Trans. Antennas Propag.*, vol. 63, no. 9, pp. 4175-4179, Sept. 2015.

[7] S. W. Qu, D. J. He, S. W. Yang, and Z. P. Nie, "Novel parasitic microstrip arrays for low-cost active phased array applications," *IEEE Trans. Antennas Propag.*, vol. 62, no. 4, pp. 1731-1737, Nov. 2014.

[8] J. Liu and Q. Xue, "Microstrip magnetic dipole Yagi array antenna with endfire radiation and vertical polarization," *IEEE Trans. Antennas Propag.*, vol. 61, no. 3, pp. 1140-1147, March 2013.

[9] J. Liu, Q. Xue, and Y.-L. Long, "4-element Yagi array of microstrip quarter-wave patch antennas," in *2013 IEEE International Wireless Symposium*, Beijing, China, April 14-18, 2013, pp. 1-4.

[10] J. Liu, D. R. Jackson, Y. L. Long," Propagation wavenumbers for half- and full-width microstrip lines in the EH_1 mode", *IEEE Trans. Microwave Theory and Techniques*, vol. 59, no.12, pp. 3005-3012, March 2011.

[11] Y.-Q Wen, B.-Z Wang, and X. Ding, "A wide-angle scanning and low sidelobe level microstrip phased array based on genetic algorithm optimization," *IEEE Trans. Antennas Propag.*, vol. 64, no. 2, pp. 805-810, Feb. 2016.

[12] I. D. H. Sáenz, R. Guinvarc'h, R. L. Haupt, and K. Louertani, "A dual-polarized wideband planar phased array with spiral antennas," *IEEE Trans. Antennas Propag.*, vol. 62, no. 9, pp. 4547-4553, Sept. 2014.

[13] I. D. H. Sáenz, R. Guinvarc'h, R. L. Haupt, and K. Louertani, "A 6:1 bandwidth, low-profile, dual-polarized ring array of spiral antennas with connecting arms," *IEEE Trans. Antennas Propag.*, vol. 64, no. 2, pp. 752-756, Feb. 2016.

[14] C.-X Mao, S. Gao, Y. Wang, F. Qin, and Q.-X. Chu, "Multimode resonator-fed dual-polarized antenna array with enhanced bandwidth and selectivity," *IEEE Trans. Antennas Propag.*, vol. 63, no. 12, pp. 5492-5499, Dec. 2015.

[15] F. Qin, S. Gao, Q. Luo, C.-X. Mao, C. Gu, G. Wei, J. Xu, J. Li, C. Wu, K. Zheng, and S. Zheng, "A simple low-cost shared-aperture dual-band dual-polarized high-gain antenna for synthetic aperture radars," *IEEE Trans. Antennas Propag.*, vol. 64, no. 7, pp. 2914-2922, July. 2016.

[16] D. S. Prinsloo, R. Maaskant, M. V. Ivashina, and P. Meyer, "A quad-mode antenna for accurate polarimetric measurements over an ultra-wide field-of-view," in *2014 8th European Conference on Antennas and Propagation* (*EuCAP*), The Hague, Netherlands, April 6-11, 2014, pp. 3260-3263.

[17] D. S. Prinsloo, R. Maaskant, M. V. Ivashina, and P. Meyer, "Mixed-mode sensitivity analysis of a combined differential and common mode active receiving antenna providing near-hemispherical field-of-view coverage," *IEEE Trans. Antennas Propag.*, vol. 62, no. 8 , pp. 3951-3961, May 2014.

[18] F. Zhu, S. Gao, A. T. S. Ho, R. A. Abd-Alhameed, C. H. See, T. W. C. Brown, J. Li, G. Wei, and J. Xu, "Ultra-wideband dual-polarized patch antenna with four capacitively coupled feeds," *IEEE Trans. Antennas Propag.*, vol. 62, no. 5, pp. 2440-2449, May 2014.

[19] N. Nakamoto, T. Takahashi, A. Ono, M. Nakashima, M. Ohtsuka, and H. Miyashita, "A dual polarized suspended stripline fed open-ended waveguide antenna subarray for phased arrays," in *2015 IEEE Antennas and Propagation (ISAP)*, Hobart, Australia, Nov. 9-12, 2016, pp. 1-4.

[20] K. Zhou, J. Yan, X. Li , X. Xuan, and Y. Liao, "Dual-polarized wideband high-efficiency phased array antenna," in *2015 IEEE 4th Asia-Pacific Conference on Antennas and Propagation (APCAP)*, Kuta, Indonesia, June30-July 3, 2015, pp. 580-581.

[21] Q. Lu, L. Gui, L. Shi, Y. Kong, and W. Chen, "An ultra-wideband dual-polarized phased array," in *2015 IEEE Asia-Pacific Microwave Conference (APMC)*, Nanjing, China, Dec. 6-9, 2015, pp. 1-3

[22] S.-T. Ko and J.-H. Lee, "Hybrid zeroth-order resonance patch antenna with broad E-plane beamwidth," *IEEE Trans. Antennas Propag.*, vol. 61, no. 1, pp. 19-25, Jan. 2013.

[23] J. G. Lee and J. H. Lee, "Zeroth order resonance loop antenna," *IEEE Trans. Antennas Propag.*, vol. 55, no. 3, pp. 994-997, Mar. 2007.